Chemical Engineering Journal 96 (2003) 37–44

Chemical Engineering Journal

www.elsevier.com/locate/cej

Generalized dynamic modeling of local heat transfer in bubble columns

Wei Chen [a], Tatsuya Hasegawa [a], Atsushi Tsutsumi [a,*], Kentaro Otawara [b], Yoshiki Shigaki [b]

[a] *Department of Chemical System Engineering, The University of Tokyo, 7-3-1 Hongo, Bunkyo-Ku, Tokyo 113-8656, Japan*
[b] *Kureha Chemical Industry, 16 Ochiai, Nishiki, Iwaki, Fukushima 974-8656, Japan*

Abstract

Instantaneous local heat transfer rates were measured by using a hot-wire probe in three bubble columns of different diameters of 200, 400 and 800 mm. The time series of heat transfer rates were analyzed by means of rescaled range (*R*/*S*) and deterministic chaos analyses. Due to the influence of highly chaotic bubble motions, the instantaneous local heat transfer exhibits low-dimensional chaotic features. The dependences of Hurst exponents and Kolmogorov entropy on the column scale consistently suggest different nonlinear hydrodynamic behaviors exist in bubble columns of different scales. Based on the measurement of instantaneous heat transfer rates, an artificial neural network (ANN) was applied to correlate instantaneous local heat transfer with dynamic motions of bubble and liquid. The ANN was optimized and trained by only using the experimental data measured at one location of 200 mm column. The trained ANN model shows good performance for the generalized use to predict the dynamic heat transfer rate in three columns over whole experimental conditions studied, indicating the ANN is capable of capturing the universal relation between instantaneous heat transfer and local bubble dynamics.

Keywords: Instantaneous heat transfer; Nonlinear analysis; Artificial neural networks; Dynamic modeling; Bubble columns

1. Introduction

Bubble columns have found wide application in a variety of chemical, biochemical and energy-related processes. One attractive feature of bubble column reactors is the high heat transfer rate. The heat transfer rate in gas–liquid flow of bubble columns is generally 100 times larger than in single phase flow [1], which favors highly exothermic and endothermic reactions. In literature, numerous studies have been devoted to understanding the heat transfer property in bubble columns. However, most of the previous work primarily focused on the time- or space-averaged heat transfer from the column wall to the bed or from the surface of an immersed heating object to the flow in laboratory- or pilot-scale columns with diameter up to 300 mm [1–7]. Little information is available for instantaneous heat transfer and its relation to the time-dependent local hydrodynamics, despite the fact that local flow structures and instantaneous contacting patterns, rather than the average hydrodynamic behaviors, have a dominant influence on the heat transfer performance in bubble columns. By measuring the instantaneous changes in heat transfer due to the passage of single gas bubble in liquid and liquid–solid system, Kumar et al. [8] observed that the bubble motion enhances heat transfer in liquid due to bubble-wake-induced turbulence. The bubble motion in bubble columns is dictated by bubble dynamics. The use of average heat transfer causes the loss of information regarding the effect of instantaneous bubble dynamics on heat transfer. This is one of the main reasons that most of the available correlations of heat transfer in bubble columns do not remain valid over the wide range of scale-up. Hence, for a comprehensive understanding of the heat transfer mechanism and more reliable modeling of the heat transfer behavior to improve design and operation of bubble column reactors, it is essential to study instantaneous heat transfer in bubble columns under wide conditions.

In recent years, attempts have been made to quantify the transient aspects and spatial inhomogeneities of complex hydrodynamic behaviors of multiphase reactors. By exploiting the deterministic chaos analysis technique, the nonlinear hydrodynamics of multiphase reactors are represented with a strange attractor reconstructed from the time series of system variables measured by specific methods. It has been recognized that bubble columns show comparable chaotic characteristics as fluidized beds [9–18], resulting from the chaotic motions of bubbles [17,18] and turbulent interaction between bubbles and the surrounding liquid medium [15]. Due to the complex spatio-temporal pattern of the dynamic flow structures, it is difficult to establish the mathematical model based on first principle for correlating the local bubble dynamics with the heat transfer characteristics.

* Corresponding author. Tel.: +81-3-5841-7336; fax: +81-3-5841-7270.
E-mail address: tsutsumi@chemsys.t.u-tokyo.ac.jp (A. Tsutsumi).

1385-8947/$ – see front matter © 2003 Elsevier B.V. All rights reserved.
doi:10.1016/j.cej.2003.08.016

Faced with the difficulties in theoretical interpretation of the relations between instantaneous heat transfer and the local bubble dynamics, we turn to the approach based on artificial neural networks (ANNs) to model the dynamic heat transfer in bubble columns. ANNs are data-drive empirical modeling tools. Their adaptability, nonlinearity and arbitrary function mapping ability make them quite suitable for complex chemical engineering problems. Since 1980s, ANNs have proven efficient in adaptive control, fault diagnosis, expert system, process modeling, estimation of thermodynamic properties [19,20], and more recently in prediction of nonlinear hydrodynamics in multiphase reactors [21–23].

In the present work, instantaneous local heat transfer rates in three bubble columns of different scales were measured by using a hot-wire probe. The rescaled range analysis and chaos analysis were applied to characterize the dynamic feature of the local heat transfer rate. An ANN-based model was proposed to model the underlying relation between the bubble dynamics and instantaneous heat transfer based on the measured time series of heat transfer rates. As a initial speculation, it is assumed that there exists some generalized relation between the local bubble dynamics and the instantaneous changes in the heat transfer rate, although the nonlinear hydrodynamics in bubble columns is very complex and may change significantly with operating conditions and columns scale. Thus, one could expect that such a model based on limited experimental data obtained in one system is capable of predicting the dynamic heat transfer characteristics in other systems of different scales far outside the range of experiments, on which the model is established.

2. Experimental

Experiments were conducted in three columns of Plexiglass with the inner diameters, of 200, 400 and 800 mm. Perforated plates with 0.5 mm holes (equilateral triangular pitch of 16 mm, opening ratio about 0.09%) were employed as the gas distributor for the three columns. Tap water and air were used as the liquid and gas phases, respectively. The height of the columns was 3 m and the static liquid level was kept at 2.0 m during the experiments. The experiments were conducted at zero liquid flow and the superficial gas velocity was varied in the range 20–90 mm/s, covering the homogeneous bubbling regime and churn turbulent regime.

The local heat transfer rate was measured by a hot-wire probe, which was developed based on the principle of the constant temperature hot-wire anemometry technique. A thin tungsten wire with a diameter of 10 μm and a length of 2.0 mm was used as a hot-wire filament. The wire was stretched between two tips of stainless supports and welded with a spot welder. A gap between the supports was exactly fixed at 2.0 mm. The supports were connected to one of the arms in the Wheatstone bridge circuit. Thus the fluctuations of the local heat transfer rate can be converted into the voltage output of the Wheatstone bridge. The hot-wire probe was mounted in three axial positions (600, 900 and 1200 mm above the distributor) and three radial positions ($r/R = 0$, 0.5 and 0.9) in the columns. The voltage signals of the hot-wire probe were recorded with a data recorder and digitized with an A/D converter at 1000 Hz. The typical acquisition time was 50 s and thus the length of time series was 50,000 points. With the heat transfer rate and temperature difference between the hot-wire filament and the bulk of the fluid in bubble columns known, the instantaneous local heat transfer coefficient can be determined.

3. Data analysis

3.1. Rescaled range (R/S) analysis

The rescaled range (R/S) analysis characterizes correlations in time series data with the Hurst exponent H. This method has already been successfully used for bubble columns with pressure fluctuation signals by Drahos et al. [14] and with optical probe signals by Kikuchi et al. [17]. When a positive correlation in time series data exists, the values of the Hurst exponent, H, are between 0.5 and 1. Higher values of H indicate that the studied data exhibit stronger persistent trend. For uncorrelated data, i.e. stochastic data, H is about 0.5. When the value of H in the range from 0 to 0.5, the data is negatively correlated. The Hurst exponent can be determined as follows. First, from the time series $x(t)$, the cumulative departure $B(t, u)$ to the average is computed in the range from $t + 1$ to $t + \tau$:

$$B(t, u) = \sum_{u=1}^{t} x(u) - \langle x \rangle_\tau \tag{1}$$

where $\langle x \rangle_\tau$ is the average value of $x(t)$ over subperiod τ. Then the sample sequential range, $R(t, \tau)$ is defined as:

$$R(t, \tau) = \max_{0 \le u \le \tau} B(t, u) - \min_{0 \le u \le \tau} B(t, u) \tag{2}$$

Finally, the rescaled range $R(t, \tau)/S(t, \tau)$, where $S(t, \tau)$ is the standard deviation calculated for subperiod τ, is a power function of τ as follows:

$$\frac{R(t, \tau)}{S(t, \tau)} \propto \tau^H \tag{3}$$

Therefore, the value of H can be evaluated from the slope of the logarithmic plot of $R(t, \tau)/S(t, \tau)$ as a function of τ.

3.2. Chaos analysis

By means of chaos analysis, the time-dependent behavior of local heat transfer rates in bubble columns can be quantified in terms of correlation dimension and Kolmogorov entropy, which are measures for dynamical degrees of freedom and for predictability of the system, respectively.

In the present study, the correlation dimension D was estimated by fitting correlation integrals calculated according

to Eq. (4) [24] to the correlation integral function defined by Eq. (5) [25]:

$$C(r)=\frac{2}{(N+1-m)(N-m)}\sum_{n=m}^{N-1}\sum_{i=0}^{N-1-n}\Theta(r-\|\vec{X}_i-\vec{X}_{i+n}\|) \quad (4)$$

$$C(r)=\left(\frac{r-r_n}{r_0-r_n}\right)^D, \quad r_n\le r\le r_0 \quad (5)$$

In Eq. (5), r_n and r_0 are the maximum noise distance and the maximum scaling distance, respectively, and Θ is the Heaviside function. The maximum norm was used to calculate the distance between two reconstructed vectors. Based on the algorithm proposed by Schouten [24,25], the sampling frequency of 1000 Hz was found to be adequate, which gives the number of point per average cycle is in the range 40–80. Embedding dimension larger than 40 and time delay equal to one sampling unit were applied reconstructing the attractor in the state space. The algorithm defined by Eq. (4) computes distances between all pairs of points except for those closer together in time than m sampling units in order to exclude dynamically correlated points from correlation integral calculation. The number of m was taken equal to that of the embedding dimension d used in the computation of correlation integral.

The maximum-likelihood approach was used to estimate the Kolmogorov entropy [26]. In this algorithm, the entropy is determined from average number of steps required for a pair of vectors, which are initially within a specific distance l_c, to separate until the distance between the vectors becomes larger than l_c.

4. Results and discussion

4.1. Dynamic analysis of instantaneous heat transfer

The representative time series of the local instantaneous heat transfer coefficient measured in bubble columns is shown in Fig. 1. It can be seen that the local heat transfer rate fluctuates vigorously, which exhibits intense rises and falls in the instantaneous changes of heat transfer coefficients. Due to the higher thermal conductivity and heat capacity, a relatively high heat transfer rate was obtained when the probe tip was immersed in the liquid phase; while the sudden dip in heat transfer coefficients was caused by the bubble passage. On the basis of significant difference in the heat transfer rate, the signal for gas and liquid phase can be identified in the time series. From the measurement of instantaneous heat transfer rates, the effects of bubble and bubble wake on the heat transfer in bubble columns are also clearly revealed. The instantaneous heat transfer coefficient begins to increase as one bubble approaches the hot-wire probe. This is due to the surface renewal caused by the approaching bubble. The bubble forces the heated liquid at the probe away from the probe and renews it with the liquid from the bulk. The local maximum instantaneous heat transfer coefficients are usually appeared in the bubble wake region due to strong local turbulence caused by the wake. This phenomenon agrees well with the observation of Kumar et al. [8] for the single bubble injection in bubbly liquid system. Moreover, it was found that much greater increase in the instantaneous heat transfer rate with the higher bubble passage frequency.

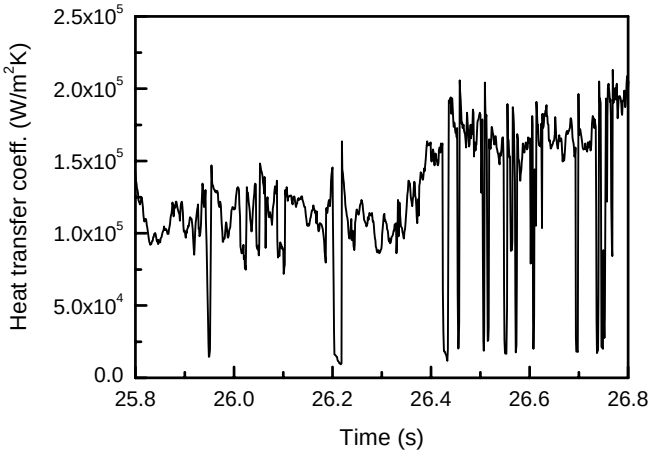

Fig. 1. Time series of instantaneous local heat transfer coefficients in bubble columns, $D = 400$ mm, $U_g = 45$ mm/s, $r/R = 0$, $h = 1.2$ m above the distributor.

The Hurst exponents obtained from the time series of instantaneous heat transfer coefficients measured in the three bubble columns are plotted in Fig. 2. As expected, for the three columns the values of H were found to be above 0.5, indicating that the local heat transfer rate in bubble columns displays persistent behaviors under the conditions examined. Since the instantaneous changes in the heat transfer rate mainly stem from the contact of the probe filament with the gas–liquid flow, the persistent behavior in the time series

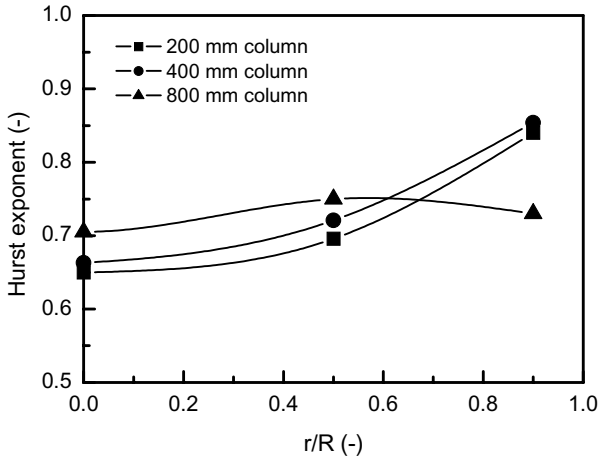

Fig. 2. Radial distribution of Hurst exponents in bubble columns, $U_g = 78$ mm/s, $h = 1.2$ m above the distributor.

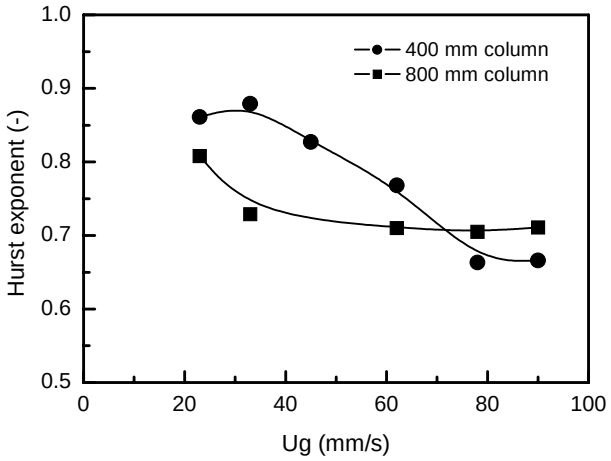

Fig. 3. Effect of gas velocity on Hurst exponents in bubble columns, $r/R = 0$, $h = 1.2$ m above the distributor.

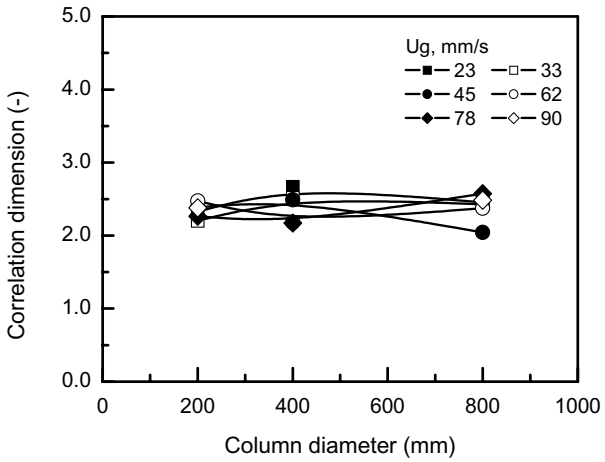

Fig. 4. Effect of column scale on the correlation dimension, $r/R = 0.0$, 1.2 m above the distributor.

of heat transfer rates can be examined based on bubble and liquid motions in bubble columns. For the 200 and 400 mm columns, the strong persistence near the wall ($r/R = 0.9$) denoted by H larger than 0.85 is attributed to the appearance of vortical structures in the vicinity of the column wall. The dynamic behavior in the central region of smaller columns is seen to be less persistent than that in the wall. This may be due to the intensive interactions between bubbles in the column center. On the contrary, in the 80 cm column the values of H show much flatter distribution. This is likely due to the existence of the column-scale circulation structure in the larger column, which will be discussed below.

Fig. 3 shows the effect of superficial gas velocity on Hurst exponents. Under low gas velocity conditions in homogeneous bubbling regime, the gas–liquid flow exhibits strong persistence. With the increase of gas velocity and accordingly the much more complexity in the gas–liquid interaction, the Hurst exponent decreases. This reveals that the tendency of the random-like motion of bubbles become significant at high gas velocities. Similar results were reported by Kikuchi et al. [17] for the R/S analysis of optical probe signals in bubble columns.

Fig. 4 shows the effect of column scale on the correlation dimension obtained from the time series of the local heat transfer rate in bubble columns. It can be seen that the instantaneous local heat transfer rate exhibits the deterministic chaotic manner with relative low correlation dimensions. No significant effect of column scale on the correlation dimension can be observed. Over the whole range of gas velocity, the correlation dimension varies between 2 and 3. On the contrary to the correlation dimension, the Kolmogorov entropy was observed to be more sensitive to the column scale. As can be seen in Fig. 5, the Kolmogorov entropies in the 200 mm column are noticeably higher than those in the 400 and 800 mm columns. This suggests the fast loss of the information and the difficulties in accurately predicting the temporal and spatial behaviors in the small-scale system. When the column diameter increases, the entropies monotonously decrease. For the 800 mm column the entropies concentrate in the range from 20 to 40 bits/s. It should be noted that different dependencies of correlation dimensions and Kolmogorov entropies on the system parameter have also been found in the CFB riser [13].

The radial distributions of the Kolmogorov entropies at 1.2 m above the distributor in the three columns are shown in Fig. 6. The same pattern, as is found for the radial distribution of Hurst exponents, is also observed here. The entropies near the wall are lower than those in the center region, especially in the smaller column. The entropy is found to be reduced with column scale in the center region and exhibits more flat radial profiles in the 800 mm column. This result is consistent with the deterministic chaos analysis to the local voidage fluctuations in bubble columns [27]. The effect of column scale on the Kolmogorov entropy could be explained by different macroscopic flow structures observed in the columns of different scales. In the columns of 200 and

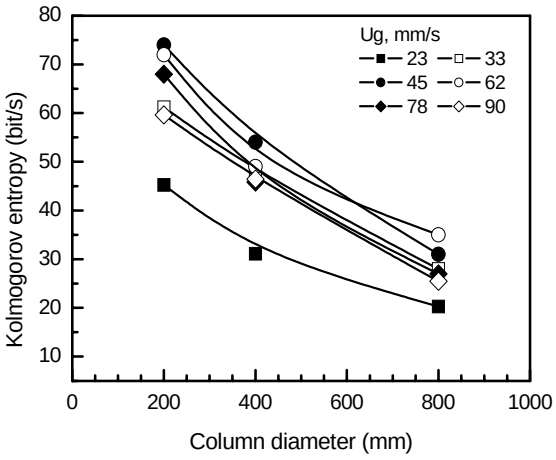

Fig. 5. Effect of column diameter on Kolmogorov entropies 1.2 m above the distributor, $r/R = 0.0$.

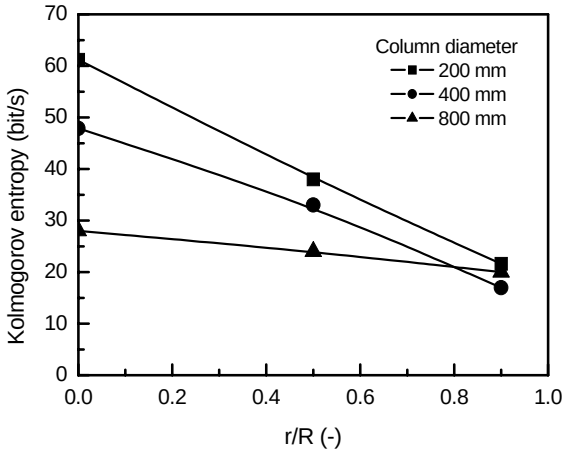

Fig. 6. Radial distribution of Kolmogorov entropies, $U_g = 33$ mm/s, 1.2 m above the distributor.

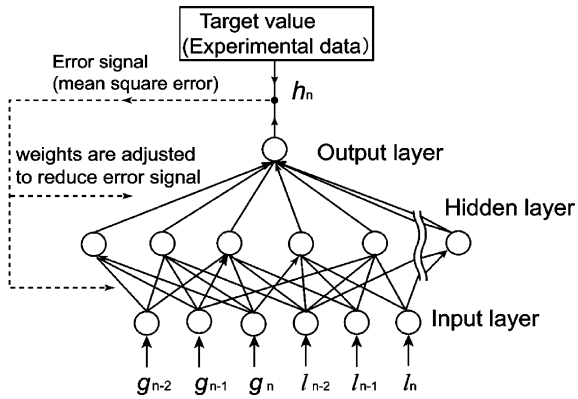

Fig. 7. Architecture of ANN model.

400 mm diameter, the bubbles were homogeneously formed at the distributor and rise up in a wavelike manner. The bubble clustering or coalescence takes places with the increase in gas velocity, forming many small vortices with scale less than the column size. On the other hand, in the 800 mm column, column-scale vortices and a gross circulation flow structure were observed. Although the gross circulation in the large-scale column does not show a regular behavior, it seems to bring more coherent structures in the flow, which could cause the reduction of the Kolmogorov entropy and a more uniform nonlinear hydrodynamic flow structure.

The significant variations in nonlinear hydrodynamic behaviors with column scale, and the corresponding variations in the dynamic feature of instantaneous local heat transfer generally indicate the methodological pitfalls involved in extrapolating correlations of average local heat transfer beyond their rang of applicability. Thus, in this work, we follow a rather simple and understandable mechanism, that in a given gas–liquid system the local bubble dynamics directly determine the instantaneous local heat transfer rate, to establish a generalized model based on ANNs for prediction of dynamic heat transfer in bubble columns.

4.2. ANN model of local dynamic heat transfer

The subject of ANNs is well covered in the literature and will not be reviewed here. Generally, the architecture of multi-layer ANNs can have many layers where a layer represents a set of parallel processing nodes. Theoretical work has shown that a single hidden layer is sufficient for ANNs to approximate any complex nonlinear function. Therefore, in this work a fully interconnected feed forward neural network containing only one hidden layer was used, as depicted in Fig. 7. Since the heat transfer rate in gas phase is far lower than in liquid phase and almost takes the same value, this ANN model was designed to predict the average heat transfer rate of liquid phase during a short interval l_n between two consecutive bubbles based on the present and past successive passage times of liquid and bubble phases, as shown in Fig. 8. The passage time of each phase reflects the local bubble dynamics in bubble columns.

The input and output nodes of the ANN used are linear, while the nodes in the hidden layers are nonlinear with sigmoidal transfer function. The training process of the ANN was carried out by using the error back-propagation algorithm and was evaluated according to the mean squared errors (MSEs) of the training data set. The way to establish the training data set is an important issue, and the quality of training data set is crucial to the success of neural network modeling. In this work, it is assumed that there exists some universal relation between the local bubble dynamics and instantaneous heat transfer in bubble columns of different scales. Hence, only the data in the time series measured in one specified position of 200 mm column under the superficial gas velocities of 23, 62 and 90 mm/s were selected to construct the training data set and validation data set for the model training. The remaining experimental data obtained in the three columns over the whole range of gas velocity were used as test data set to examine the prediction capability of the proposed ANN model, especially in the scale-up application. The experimental conditions for training data set and test data set are listed in Tables 1 and 2, respectively.

Table 1
Experimental conditions for the training data set for the ANN model

Column diameter (mm)	200
Measurement position	
Axial height above distributor (mm)	900
Radial position, r/R	0.0
Gas velocity (mm/s)	23, 62 and 90

Table 2
Experimental conditions for the test data set for the ANN model

Column diameter (mm)	200, 400 and 800
Measurement position	
Axial height above distributor (mm)	600, 900 and 1200
Radial position, r/R	0.0, 0.5 and 0.9
Gas velocity (mm/s)	23, 33, 45, 62, 78 and 90

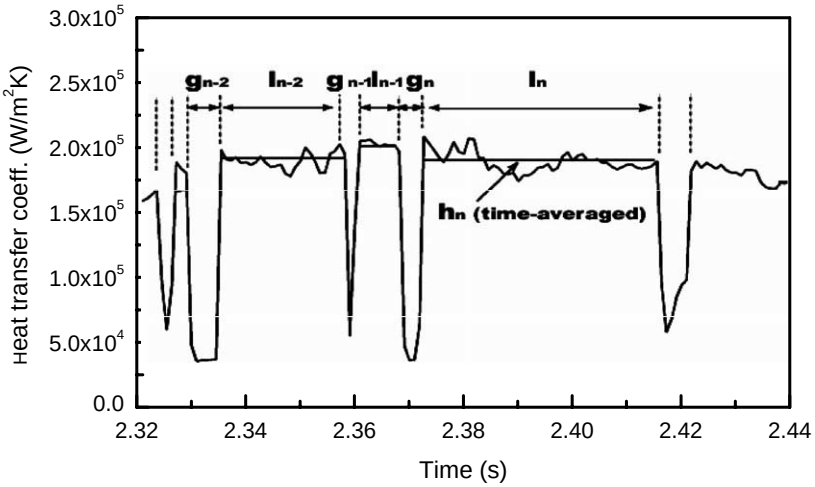

Fig. 8. Data preparation for the ANN model.

Since so far there is no rigorous theoretical method for the determination of the architecture of ANNs, the trial-and-error process was adopted for network design. To identify an appropriate ANN model, the number of input nodes was varied from 2 to 8, and hidden nodes from 5 to 50. The fit to the validation data set was evaluated by MSE. As illustrated in Fig. 9, with hidden nodes of 10, using 6 and 8 input nodes provides comparably lower validation error. In this case, the network with small number of essential nodes is preferable. Thus, the number of input and hidden nodes are chosen to be 6 and 10 for the ANN used in this work. In this ANN model, the number of input layer nodes is associated with the manner in which the time-dependent bubble motions affect local heat transfer. The optimum number of input nodes was found to be 6. This means that the present heat transfer rate of liquid phase is significantly dependent on the motions of past three bubbles.

4.3. Evaluation of the ANN model

After well trained, the prediction performance of the ANN model was examined using the never-seen-before data of test data set. A typical comparison of the predicted and measured heat transfer coefficients is shown in Fig. 10. Note that the predicted values for liquid phase are outputs of the ANN model while for gas phase the average value of measurement results is simply plotted as the predicted value. From this figure, it can be seen that the predicted heat transfer coefficients approach well to the measured ones. This result suggests that the ANN model does not memorize but accurately capture the underlying relationship between instantaneous heat transfer and the local bubble dynamics.

The prediction error distributions of the ANN model for the three columns are presented in Fig. 11(a)–(c). Although, as mentioned above, different macroscopic flow

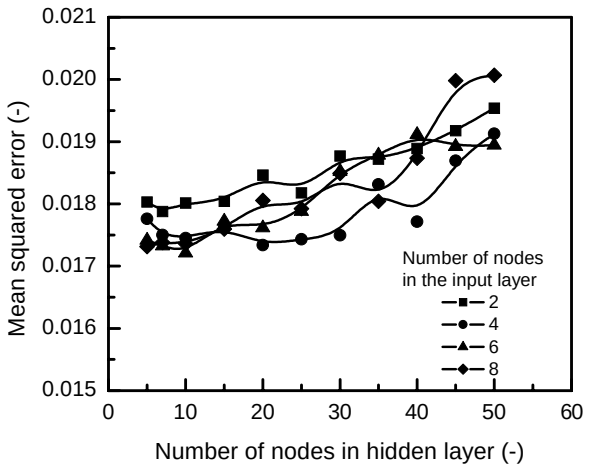

Fig. 9. Optimization of the number of nodes in the neural network.

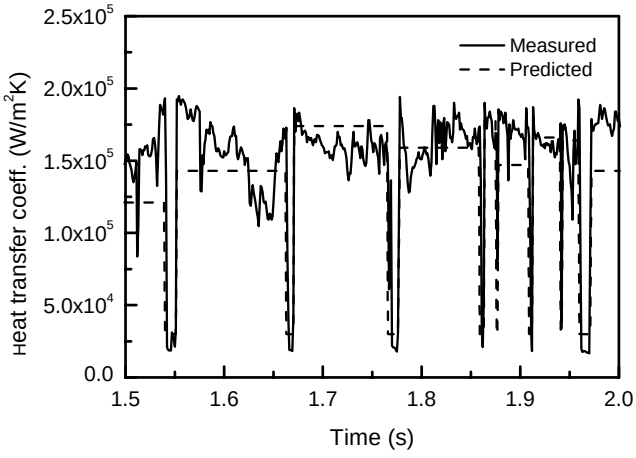

Fig. 10. The comparison of measured and predicted heat transfer coefficients using ANN model in 200 mm column, $U_g = 45$ mm/s, axial position = 900 mm, radial position, $r/R = 0$.

structure and nonlinear hydrodynamic behaviors exist in bubble columns of different scale, over the whole range of our experiments, it can be seen that the prediction error distributions for the three columns are similar, nearly following the normal distribution. The column size and the variation of locations do not produce any pronounced changes in the prediction capability of the ANN model. From Fig. 11, the average errors between the predicted and measured heat transfer coefficients in the three columns are all less than 3%. To get a much clearer illustration, the parity plot of predicted versus measured average heat transfer coefficients for the three columns is shown in Fig. 12. The predicted average local heat transfer coefficients at different locations in the three columns are in good agreement with the measured ones within 10% relative error.

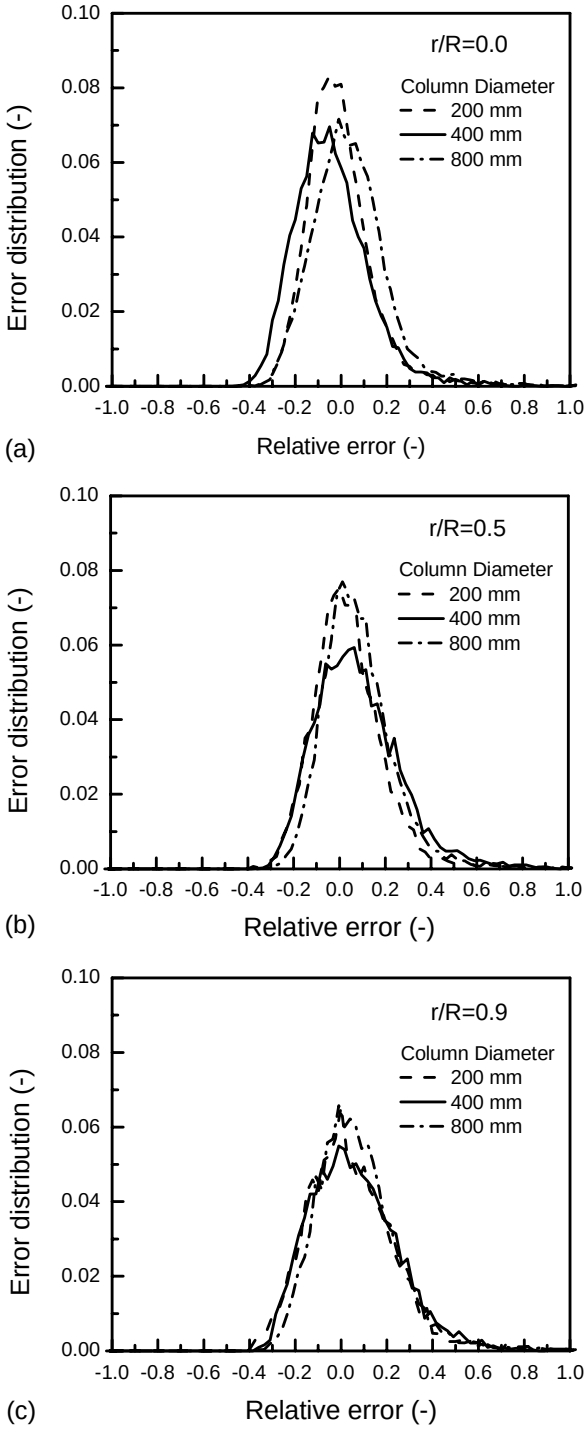

Fig. 11. The distributions of prediction error of ANN model.

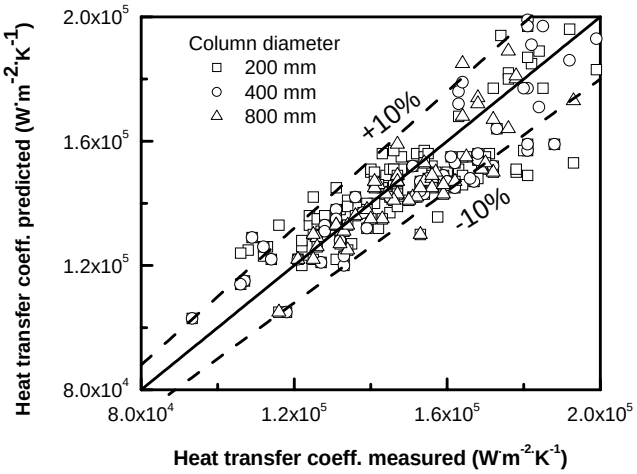

Fig. 12. Parity plot of predicted versus measured average heat transfer coefficients.

These results confirm that there exists universality of the relationship between the local bubble dynamics and the instantaneous heat transfer rate. More importantly, it is shown that only very limited data, as the training data used in this work, could be good representative of the universal relation and form the necessary basis for modeling. A dynamic model gaining an insight into such a relation holds high possibility for the generalized use in the scale-up and design of bubble column reactors.

5. Conclusions

By using a hot-wire probe, the instantaneous local heat transfer rates were measured at various axial and radial positions in three bubble columns of different scales. The rescaled range analysis and deterministic chaos analysis were applied to characterize the dynamic features of instantaneous heat transfer. Because the heat transfer behavior is predominantly determined by the local bubble dynamics, the instantaneous heat transfer rate measured reflects the nature of nonlinear hydrodynamics in bubble columns. The analyses show local dynamic heat transfer in bubble column appears low-dimensional chaotic characteristics with the correlation dimension in the range 2–3. Both the variations of Hurst exponents and Kolmogorov entropies with column scale suggest that different nonlinear hydrodynamic behaviors exist in bubble columns of different scales.

Based on the time series of instantaneous heat transfer rates measured, an ANN-based model was proposed to

correlate the local bubble dynamics and instantaneous heat transfer. It was demonstrated that the ANN-based model only trained with the dynamic data obtained from one specified location in 200 mm column is capable of predicting the instantaneous local heat transfer rates of different locations in bubble columns with diameter up to 800 mm. This reveals that the trained ANN can generalize the fundamental relationship between local heat transfer and bubble dynamics in bubble columns. Considering the difficulties in theoretical interpretation of the relations between local instantaneous heat transfer with the local bubble dynamics, the dynamic heat transfer model based on ANN presents a valuable success and can be a effective computational tool for the direct correlation of chaotic gas–liquid behavior with the transport phenomena in bubble columns.

Acknowledgements

The authors would like to thank the financial support of a “Core Research for Evolutional Science and Technology” grant from the Japan Science and Technology Corporation (JST).

References

[1] W.D. Deckwer, On the mechanism of heat transfer in bubble column reactors, Chem. Eng. Sci. 35 (1980) 1341–1346.
[2] C.G.J. Baker, E.R. Armstrong, M.A. Bergougnou, Heat transfer in three-phase fluidized bed, Powder Technol. 21 (1978) 195–204.
[3] Y. Kato, K. Uchida, K. Kago, S. Morooka, Liquid holdup and heat transfer coefficient between bed and wall in liquid–solid and gas–liquid–solid fluidized beds, Powder Technol. 28 (2) (1981) 173–179.
[4] K. Muroyama, M. Fukuma, A. Yasunishi, Wall-to-bed heat transfer coefficient in liquid–solid and gas–liquid–solid fluidized beds, Can. J. Chem. Eng. 64 (1986) 399.
[5] S.C. Saxena, Heat transfer from a cylindrical probe immersed in a bubble column, Chem. Eng. J. 41 (1989) 25–39.
[6] S.C. Saxena, N.S. Rao, Heat transfer and gas holdup in a two-phase bubble column: air–water system-review and new data, Exp. Therm. Fluid Sci. 4 (1991) 139–151.
[7] L.-S. Fan, Gas–Liquid–Solid Fluidization Engineering, Butterworths, Stoneham, MA, 1989, pp. 163–249.
[8] S. Kumar, K. Kusakabe, K. Raghunathan, L.S. Fan, Mechanism of heat transfer in bubbly liquid and liquid–solid systems: single bubble injection, AIChE J. 38 (5) (1992) 733–741.
[9] C.S. Daw, J.S. Halow, Evaluation and control of fluidization quality through chaotic time series analysis of pressure drop measurements, AIChE Symp. Ser. 89 (1993) 103–122.
[10] C.M. van den Bleek, J.C. Schouten, The fluidized bed as a deterministic chaotic system, Chem. Eng. J. 53 (1993) 75–87.
[11] J.X. Bouillard, A.L. Miller, Experimental investigation of chaotic hydrodynamic attractor in circulating fluidized bed, Powder Technol. 79 (1994) 211–215.
[12] C.L. Briens, J.M. Hay, C. Hudson, Correlation dimension for a gas–liquid contactor, Chem. Eng. J. 64 (1996) 157–167.
[13] A. Marzocchella, R.C. Zijerveld, J.C. Schouten, C.M. van den Bleek, Chaotic behavior of gas–solids flow in the riser of a laboratory-scale circulating fluidized bed, AIChE J. 43 (6) (1997) 1458–1468.
[14] J. Drahos, F. Bradka, M. Puncochar, Fractal behaviour of pressure fluctuations in a bubble column, Chem. Eng. Sci. 15–16 (1992) 4069–4075.
[15] K. Nguyen, C.S. Daw, P. Chakka, M. Cheng, D.D. Bruns, C.E.A. Finney, M.B. Kennel, Spatio-temporal dynamics in a train of rising bubbles, Chem. Eng. J. 64 (1996) 191–197.
[16] H.M. Letzel, J.C. Schouten, R. Krishna, C.M. van den Bleek, Characterization of regimes and regime transitions in bubble columns by chaos analysis of pressure signals, Chem. Eng. Sci. 52 (24) (1997) 4447–4459.
[17] R. Kikuchi, T. Yano, A. Tsutsumi, K. Yoshida, M. Punchochar, J. Drahos, Diagnosis of chaotic dynamics of bubble motion in a bubble column, Chem. Eng. Sci. 52 (1997) 3741–3745.
[18] W. Luewisuthichat, A. Tsutsumi, K. Yoshida, Bubble characteristics in multi-phase flow systems: bubble sizes and distributions, J. Chem. Eng. Jpn. 30 (1997) 461–466.
[19] A.J. Morris, G.A. Montague, M.J. Willis, Artificial neural networks: studies in process modelling and control, Trans. IChemE, Part A 72 (1994) 3–19.
[20] D.R. Baughman, Y.A. Liu, Neural Networks in Bioprocessing and Chemical Engineering, Academic Press, San Diego, CA, 1995.
[21] R. Bakker, R.J. De Korte, J.C. Schouten, C.M. van den Bleek, Neural networks for prediction and control of chaotic fluidized bed hydrodynamics: a first step, Fractals 5 (3) (1997) 523–530.
[22] K. Otawara, L.T. Fan, A. Tsutsumi, K. Yashida, An artificial neural network as a model for chaotic behavior of a three-phase fluidized bed, Chaos, Solitons Fractals 13 (2002) 353–362.
[23] H.Y. Lin, W. Chen, A. Tsutsumi, Long-term prediction of nonlinear hydrodynamics in bubble columns by using artificial neural networks, Chem. Eng. Proc. 42 (8–9) (2003) 611–620.
[24] J. Theiler, Estimation fractal dimension, J. Opt. Soc. Am. A 7 (1990) 1055–1073.
[25] J.C. Schouten, F. Takens, C.M. van den Bleek, Estimation of the dimension of a noisy attractor, Phys. Rev. E 50 (1994) 1851–1861.
[26] J.C. Schouten, F. Taken, C.M. van den Bleek, Maximum-likelihood estimation of the entropy of an attractor, Phys. Rev. E 49 (1994) 126–129.
[27] T. Yano, K. Kuramoto, A. Tsutsumi, K. Otawara, Y. Shigaki, Scale-up effects in nonlinear dynamics of three-phase reactors, Chem. Eng. Sci. 54 (21) (1999) 5259–5263.